

## Characteristics of the ionospheric variability as a function of season, latitude, local time, and geomagnetic activity

E. A. Araujo-Pradere, T. J. Fuller-Rowell, and M. V. Codrescu

Cooperative Institute for Research in Environmental Sciences, University of Colorado, and Space Environment Center,  
NOAA, Boulder, Colorado, USA

D. Bilitza

Raytheon ITSS/NASA Goddard Space Flight Center, Greenbelt, Maryland, USA

Received 27 September 2004; revised 2 June 2005; accepted 14 July 2005; published 18 October 2005.

[1] An ionospheric  $F_2$  critical frequency database has been assembled to determine the variability of the  $F$  region as a function of local time, latitude, season, and geomagnetic activity. The database comprises observations from 75 ionosonde stations covering a range of geomagnetic latitude and includes 43 storm intervals. The database was previously used to develop the Storm-Time Empirical Ionospheric Correction Model (STORM). The mean and standard deviation have been evaluated by sorting the data by local time, season (five intervals centered on equinox, solstice, and intermediate intervals), latitude (four regions each  $20^\circ$  wide in geomagnetic latitude), and up to eight levels of geomagnetic activity. The geomagnetic activity index was based on a weighted integral of the previous 33 hours of  $ap$  and is the same as that used by the STORM model. The database covers a full solar cycle, but insufficient information was available to sort by solar activity without compromising the estimates of variability on the other sorting parameters. About half the data were contained in the first level of geomagnetic activity, between 0 and 500 units of filtered  $ap$  corresponding to  $Kp \leq 2$ , and half above that level. When local time dependence was included in the binning, sufficient data were available to sort into two levels of geomagnetic activity, quiet ( $Kp \leq 2^+$ ) and disturbed ( $Kp > 3^-$ ). For all latitudes and levels of geomagnetic activity, the lowest variability was typically found in summer (10–15%), and the largest variability occurred in winter (15–40%), with equinox (10–30%) lying between the solstice extremes. The exception was low latitudes at equinox, which had surprising low variability (10%), possibly because of the weak interhemispheric flow at this time of year. At middle and low latitudes, the variability tended to increase with geomagnetic activity in winter and equinox but remained fairly constant in summer. At high latitudes, the surprising result was that in all seasons, and in winter in particular, the variability tended to decrease, probably because of the increased upwelling of neutral molecular species and stronger chemical control of the ionosphere. The data have also been used to build a table of estimated variability suitable for inclusion in the International Reference Ionosphere or any other climatological model. For periods where data were scarce or nonexistent, an estimated variability was provided on the basis of expectations of the consequences of physical processes. This was necessary to fill in the table of values in order to develop a module suitable for inclusion in the International Reference Ionosphere.

**Citation:** Araujo-Pradere, E. A., T. J. Fuller-Rowell, M. V. Codrescu, and D. Bilitza (2005), Characteristics of the ionospheric variability as a function of season, latitude, local time, and geomagnetic activity, *Radio Sci.*, 40, RS5009, doi:10.1029/2004RS003179.

## 1. Introduction

[2] Several physics-based models are successful in describing the ionospheric behavior during quiet and perturbed conditions. Among them are the Time Dependent Ionospheric Model (TDIM) [Schunk et al., 1986], the Coupled Thermosphere-Ionosphere Models (CTIM and CTIP) [Fuller-Rowell et al., 1987, 1996; Millward et al., 1996; Quegan et al., 1982], and the NCAR Thermosphere-Ionosphere Global Circulation Models (TIGCM and TIEGCM) [Roble et al., 1988; Richmond et al., 1992]. The quiet state of the ionosphere is also well described by several empirical models, the best known being the International Reference Ionosphere (IRI) [Bilitza, 2001].

[3] The IRI is an international project sponsored by the Committee on Space Research (COSPAR) and the International Union of Radio Science (URSI). The IRI is based on data and captures much of the repeatable characteristics of the ionospheric during both quiet and storm-time periods. The quiet-time ionosphere depends on solar activity, season, latitude, longitude, and local time. Recent additions now also include dependence on geomagnetic activity. For a specified setting (location, time, date, and  $ap$  time history) IRI provides monthly medians for magnetically quiet conditions, together with a correction for storm times for the  $F$  region.

[4] The complexity of the processes involved in storm conditions makes it harder to model the ionospheric response to disturbed conditions. Several attempts have been made in both physically based and empirical models. In IRI 2001 the disturbed conditions use the Storm-Time Empirical Ionospheric Correction Model (STORM), an empirical model driven by the previous time history of  $ap$ , which is designed to scale the quiet-time  $F$  layer critical frequency ( $f_oF_2$ ) or peak concentration ( $NmF_2$ ) to account for storm-time changes in the ionosphere. The design of the STORM model contains the seasonal dependence due to the migration of the composition bulge by the global wind field, latitude dependence, and a nonlinear dependence on the integrated time history (over 33 hours) of  $ap$  (for a detailed discussion of the integral of  $ap$ , or filtered  $ap$ , see Araujo-Pradere et al. [2002] and Fuller-Rowell et al. [2001]).

[5] The STORM model has been extensively validated [Araujo-Pradere and Fuller-Rowell, 2001, 2002], as has the response of IRI2001 for storm conditions [Araujo-Pradere et al., 2003a, 2003b]. In general, the STORM model improves the prediction of IRI 2001 up to 50% when compared with IRI 1995 (with no storm correction).

[6] IRI 2001 currently does not include estimates of uncertainty or variability surrounding the mean values. The present work is designed to add this feature. The standard deviations have been used to describe the geophysical variability of the data. For each bin of local time, latitude, and season, the standard deviation and the population distribution were obtained for varying levels of geomagnetic activity. Part of this work was recently published [Araujo-Pradere et al., 2004a] but has been extended in the present paper by including the discussion of the local time dependence. With the local time dependence included, we present results for two levels of geomagnetic activity, quiet ( $Kp \leq 2^+$ ) and disturbed ( $Kp > 3^-$ ). The intervals selected for this initial study on variability also covered a range of solar activity, but it was deemed that the volume of the data analyzed so far was insufficient to add this sorting parameter without compromising the statistics for the other variables. This variability information is currently being used to estimate the uncertainty in the storm-time prediction provided by the Real Time STORM (RT-STORM), an operational product at the NOAA Space Environment Center (<http://sec.noaa.gov/storm/>). This information can also be used to characterize the ionospheric variability as a part of the IRI or any other climatological model.

## 2. Data Sources

[7] Ionosonde data were selected covering quiet and disturbed periods, a range of seasons, and from a sufficient number of stations to provide a reasonable spread in geomagnetic latitude. The data used were the  $f_oF_2$  hourly values for each site, and the integral of  $ap$ , to describe the geomagnetic activity. This index is designed to weight the time history of the activity and is obtained applying a 33-hour filter obtained by the singular value decomposition method. The integral of  $ap$  is related to the  $Dst$  index by  $Dst = -0.07(\text{integral of } ap) - 1.45$ , with a correlation of 0.78. Although not a perfect correlation, the relationship is reasonably linear and enables the integral of  $ap$  to be related to the more familiar measure of the magnitude of a storm [Araujo-Pradere et al., 2002].

[8] The data selected covered storm periods and the quiet days preceding the storms. More than half the data analyzed were for  $Kp \leq 2$ . All the ionospheric data were obtained from the NOAA-NGDC Space Physics Interactive Data Resource (SPIDR, <http://spidr.ngdc.noaa.gov/>). The intervals selected roughly comprised a full

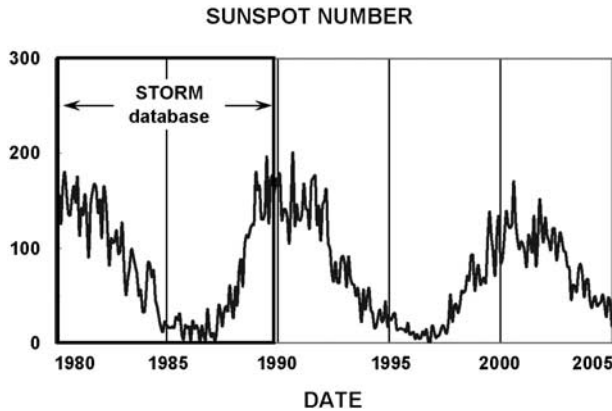


**Figure 1.** Data included in the STORM database, roughly covering a solar cycle.

solar cycle (all storms in the period 1981–1988, depicted by the framed part of Figure 1).

[9] Some of the data during storm periods may be affected by cases where the  $F_2$  peak is below that of  $F_1$ . These cases are included in the statistics and, although rare, will have a modest impact on the estimation of variability.

[10] Rather than analyze the variability for every month, the data were grouped into five seasonal periods: summer, winter, equinox, and intermediate periods, each covering approximately 45 days. The new intermediate seasons (described in detail by Araujo-Pradere *et al.* [2004a]) cover the dates between winter solstice and the equinox (21 October to 21 November and 21 January to 21 February at the Northern Hemisphere) and summer solstice and the equinox (21 April to 21 May and 21 July to 21 August at the Northern Hemisphere).

[11] The intervals selected covered a range of seasons: 7 occurred during the equinoxes, 11 during peak solstices, and 7 during the previously described intermediate periods. The database incorporates 25 storms (from June 1981 to June 1988), with an average of 75 stations per storm, with a coverage extending from Resolute Bay, at  $83.2^\circ\text{N}$  of geomagnetic latitude (GMLat), to Scott Base at  $78.8^\circ\text{S}$  GMLat. A detailed list of storms and stations can be found in work by Araujo-Pradere *et al.* [2002].

### 3. Results

#### 3.1. Seasonal Latitudinal Dependence

[12] Figure 2 shows the standard deviation about the mean of the normalized  $F_2$  critical frequency as a function of latitude, season, and geomagnetic activity. Data from all the local times have been combined in the analysis shown in Figure 2. The abscissa, or  $x$  axis, in

each plot is the integral of the  $ap$  index, and the ordinate, or  $y$  axis, corresponds to the ratio between the observed and the monthly mean values of  $foF_2$  ( $\Phi = foF_{2obs}/foF_{2mm}$ ). In each plot a polynomial cubic fit to the data has been determined, and the standard deviation centered about this fit describes the geophysical variability for the particular conditions (i.e., season, geomagnetic latitude, or level of geomagnetic activity). The variability is either calculated from observations in the cases where sufficient data is available or is estimated on the basis of physical interpretation in cases where insufficient or no data are available. An extensive discussion of the ionospheric response appears in the aforementioned articles; here we will offer a very short review of this topic (in order to assess the feasibility of the database), but we will mainly focus on the analysis of the variability of the data. Note that the sample of data available during periods of disturbed geomagnetic activity was sometime sparse and sometimes even nonexistent. In these cases, values of both the mean and standard deviation had to be estimated either by interpolation, extrapolation, or by imposing scientific judgment.

[13] In Figure 2, the data show a consistent decrease in the mean as a function of geomagnetic activity for most of the latitude bands in the summer hemisphere, whereas the winter hemisphere presents a more complex behavior. The theory of the response of the global circulation to geomagnetic storms [Roble, 1986] suggests that a boundary will exist between the positive and negative ionospheric response at around  $40^\circ$  GMLat [Araujo-Pradere *et al.*, 2004b]. This boundary is reflected in the sorted data. The ionospheric response for the equinox season resembles the summer response, with a consistent negative phase that increases with geomagnetic latitude. The summer intermediate seasons also present a similar response to that of the summer, while the winter intermediate differs from the winter season in the direction and shape, with the exception of high latitudes.

[14] Figure 2 also shows a clear difference between the variability in summer and winter. Summer and equinox show a fairly consistent behavior, with a gradual decrease in the mean as geomagnetic activity increases, the scatter of points being fairly tightly grouped. The winter and winter intermediate are less coherent, with data points widely, but not regularly, dispersed around the proposed model. It is possible to see that for both these seasons, at midlatitudes (20–40 and 40–60), there are several points dispersed toward the higher values (positive response) even when the general trend on the mean is to the negative response (a clear illustration of this is seen in the winter intermediate season, 40–60° GMLat, between 2000 and 3000 units of the integral of  $ap$ ). This dissimilar behavior of part of the population with respect to the main trend will be explored further.

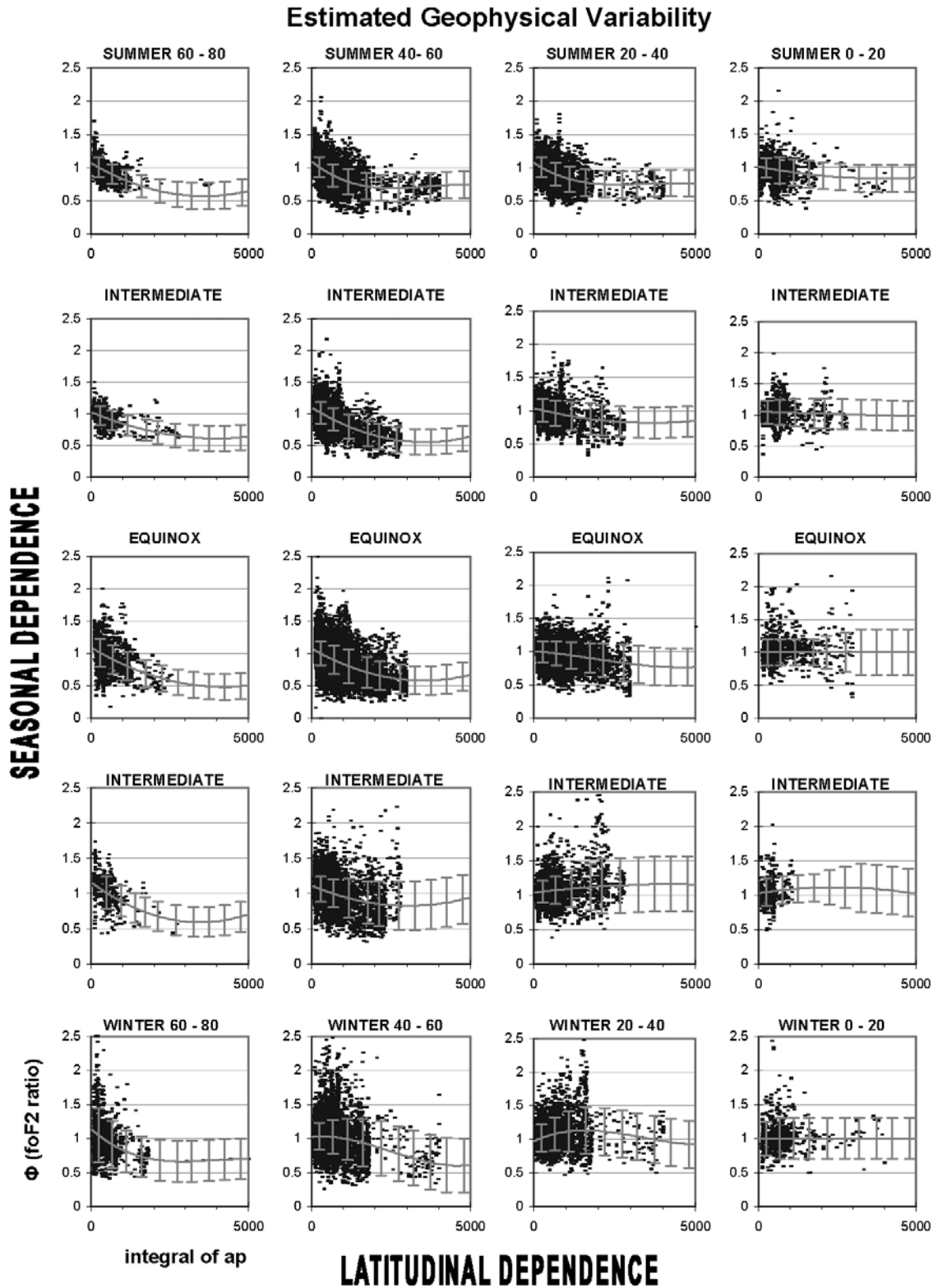


Figure 2

[15] In all bins, the standard deviation quantifies the geophysical variability. There are two representations of the variability in this work and the results of both listed in Table 1. The first corresponds to the case where enough data existed. In this case, a straightforward calculation of the standard deviation provided the value of the variability for the corresponding bin (labeled as “Observed” in Table 1). For the second case, regions where observations were scarce or nonexistent, the observed variability was adjusted, or filled in, by imposing scientific judgment on the basis of expectations of the consequences of physical processes (“Estimated” in Table 1). Figure 2 shows the regions of missing data where values have to be estimated. For example, for winter 20–40° GMLat, we expected the variability to continue high because of the stronger influence of dynamics, whereas for summer, at the same bin of GMLat, we expected the variability to be more constrained because of the greater control by chemical processes.

[16] Table 1 shows the observed and estimated geophysical variability covering the seasons from summer to winter. The first column shows the level of geomagnetic activity expressed by the integral of  $ap$ , and the following columns show either the observed or estimated geophysical variability for each latitudinal band as a function of geomagnetic activity. The estimated variability is used in the operational version of the RT-STORM model for the calculation of the error bars and could be applied to any reference model. Note that all local times have been combined in these estimates, so the values represent a diurnal average.

[17] The cells in the observed variability of Table 1 that contain no values correspond to regions of nonexistent data. Some of the observed values are also affected by limited data, which compromises the description of the true ionospheric variability and need to be adjusted. Good examples of this case are the high latitudes of summer at activity level 4000 and winter and summer intermediates at 3000 units of the integral of  $ap$ , where the observed variability is exceptionally low: 0.01, 0.07, and 0.04, respectively. Figure 2 shows that the data contained in these three regions are particularly scarce, so the values obtained are unlikely to be representative of the true ionospheric variability. However, there is the technical possibility that for large integral of  $ap$  the exceptionally low variability may be a true reflection of the observations. These cases may be periods when  $foF_2$  is less than  $foF_1$  and therefore is replaced by  $foF_1$  in tabulations. Using  $foF_1$  in place of  $foF_2$  will tend to lead

to an underestimation of the variability of the  $F_2$  layer itself.

[18] An interesting feature is the increasing variability for the midlatitudes of winter and winter intermediate, between 1500 and 3000 units of the filtered  $ap$ , where the variability is twice that of both summer and equinox. This increased variability is due to the difference between the circulation patterns in summer and winter and the impact of the storm circulation. The so-called “solar-driven circulation” generates, for quiet geomagnetic conditions, a latitudinal profile of the mean molecular mass with a maximum in the summer high latitudes and a minimum in the winter hemisphere. The high-latitude geomagnetic/magnetospheric energy sources assist this trend in summer and compete in winter. In winter, a boundary is created near 40° geomagnetic latitude between the positive and negative phases of the storm response [Araujo-Pradere *et al.*, 2004b]. The movement of this boundary in the data is reflected in the increased variability in winter midlatitudes.

### 3.2. Empirical Distributions

[19] Figure 3 explores the characteristics of the distributions of variability and the possible causes of the various shapes. Figure 3 includes all seasons for 20–40°, on the right side, and 40–60°, on the left side, bins of geomagnetic latitude, from summer at the top to winter at the bottom, including the intermediate seasons. The data have been divided into four levels of geomagnetic activity, 0–500, 500–1000, 1000–2000, and 2000–4000, for the integrated  $ap$ , where the legend of the top right plot identifies the level of geomagnetic activity corresponding to each line in all plots. In Figure 3, the abscissa corresponds to the range of  $\Phi$  values ( $\Phi = foF_2_{obs}/foF_2_{mm}$ ) in 0.1 steps. The midpoint ( $\Phi = 1$ ) is the monthly mean for quiet conditions, and greater or lower values correspond to positive or negative phase of the storms, respectively. The ordinate describes the percentage of data points in each range of values.

[20] It is possible to obtain from Figure 3 a general indication about the distributions. More specific information is provided in Tables 2a and 2b, in order to quantify the degree to which the distributions depart from a normal or Gaussian shape. However, a common feature is the shifting of all distributions, for higher levels of activity, to a mean other than 1, reflecting the negative and positive phases of the ionospheric response.

**Figure 2.** Sort of the storm-time ionospheric response into four geomagnetic latitude bins and five seasonal bins, including intermediate seasons. Each plot shows the relationship between the  $foF_2$  ratio and the integral of  $ap$ . The error bars represent the estimated geophysical variability. See color version of this figure in the HTML.

**Table 1.** Observed and Physically Interpreted Estimates of Geophysical Variability

Integral of $ap$	Observed				Estimated			
	80–60° GMLat	60–40° GMLat	40–20° GMLat	20–00° GMLat	80–60° GMLat	60–40° GMLat	40–20° GMLat	20–00° GMLat
	<i>Summer</i>							
500	0.14	0.14	0.14	0.14	0.15	0.15	0.15	0.15
1000	0.10	0.15	0.16	0.19	0.15	0.17	0.17	0.20
1500	0.14	0.18	0.18	0.19	0.16	0.19	0.19	0.20
2000	0.17	0.18	0.17	0.17	0.17	0.20	0.20	0.20
2500	-	0.17	0.18	0.10	0.18	0.20	0.20	0.20
3000	-	0.19	0.16	0.05	0.19	0.20	0.20	0.20
3500	-	0.23	0.16	0.09	0.20	0.20	0.20	0.20
4000	0.01	0.08	0.12	0.08	0.20	0.20	0.20	0.20
4500	-	-	-	-	0.20	0.20	0.20	0.20
5000	-	-	-	-	0.20	0.20	0.20	0.20
	<i>Intermediate S-E</i>							
500	0.12	0.16	0.14	0.17	0.15	0.17	0.17	0.18
1000	0.10	0.17	0.18	0.20	0.15	0.18	0.19	0.20
1500	0.12	0.15	0.22	0.14	0.16	0.19	0.21	0.22
2000	0.15	0.20	0.24	0.21	0.17	0.20	0.23	0.24
2500	0.17	0.15	0.21	0.24	0.18	0.20	0.23	0.24
3000	0.04	0.11	0.11	0.08	0.19	0.20	0.23	0.24
3500	-	-	-	-	0.20	0.20	0.23	0.24
4000	-	-	-	-	0.20	0.20	0.23	0.24
4500	-	-	-	-	0.20	0.20	0.23	0.24
5000	-	-	-	-	0.20	0.20	0.23	0.24
	<i>Equinoxes</i>							
500	0.21	0.17	0.12	0.18	0.22	0.18	0.16	0.20
1000	0.21	0.21	0.15	0.19	0.22	0.22	0.18	0.20
1500	0.20	0.26	0.17	0.17	0.22	0.26	0.20	0.20
2000	0.14	0.21	0.21	0.16	0.21	0.24	0.22	0.20
2500	0.13	0.21	0.24	0.44	0.20	0.22	0.25	0.25
3000	-	0.20	0.27	0.36	0.20	0.22	0.28	0.30
3500	-	-	-	-	0.20	0.22	0.28	0.35
4000	-	-	-	-	0.20	0.22	0.28	0.35
4500	-	-	-	-	0.20	0.22	0.28	0.35
5000	-	-	-	-	0.20	0.22	0.28	0.35
	<i>Intermediate E-W</i>							
500	0.22	0.17	0.15	0.19	0.23	0.18	0.16	0.20
1000	0.21	0.20	0.19	0.13	0.22	0.20	0.20	0.20
1500	0.21	0.28	0.32	0.21	0.21	0.28	0.27	0.20
2000	0.11	0.30	0.39	-	0.21	0.30	0.34	0.20
2500	-	0.35	0.47	-	0.21	0.32	0.40	0.25
3000	0.07	0.44	0.13	-	0.21	0.34	0.40	0.30
3500	-	-	-	-	0.21	0.35	0.40	0.35
4000	-	-	-	-	0.21	0.35	0.40	0.35
4500	-	-	-	-	0.21	0.35	0.40	0.35
5000	-	-	-	-	0.21	0.35	0.40	0.35
	<i>Winter</i>							
500	0.33	0.19	0.14	0.22	0.40	0.20	0.20	0.25
1000	0.20	0.26	0.18	0.19	0.35	0.25	0.25	0.30
1500	0.32	0.27	0.26	0.27	0.30	0.30	0.30	0.30
2000	0.13	0.26	0.43	0.19	0.30	0.35	0.35	0.30
2500	-	0.33	0.23	0.09	0.30	0.40	0.35	0.30
3000	-	0.59	0.24	0.06	0.30	0.40	0.35	0.30
3500	-	0.16	0.18	0.27	0.30	0.40	0.35	0.30
4000	-	0.38	0.25	0.26	0.30	0.40	0.35	0.30
4500	-	-	-	-	0.30	0.40	0.35	0.30
5000	-	-	-	-	0.30	0.40	0.35	0.30

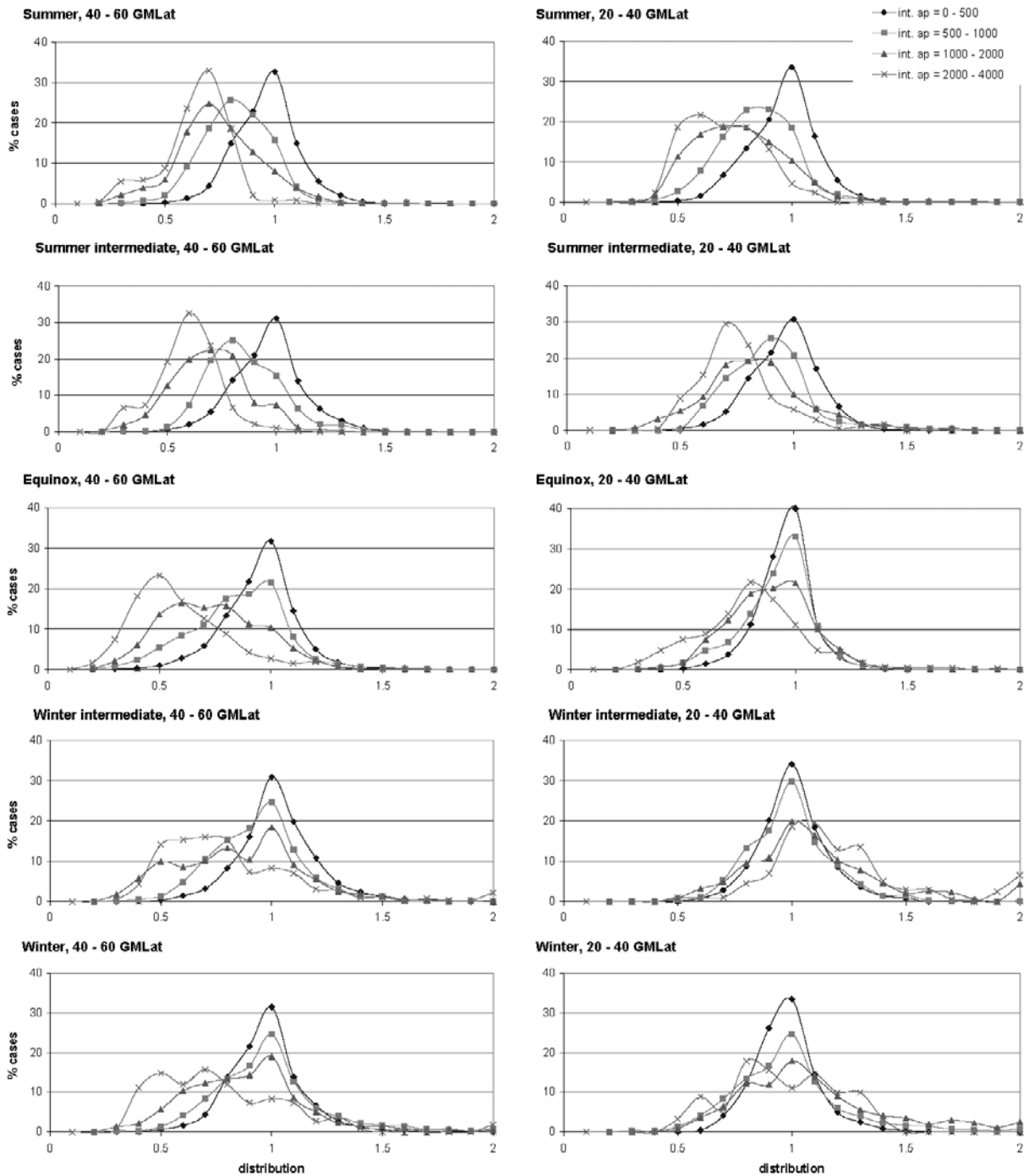


**Figure 3.** Examples of the distribution of data points as a function of the values for midlatitude (20–40° and 40–60° GMLat) for all seasons. See color version of this figure in the HTML.

**Table 2a.** Distribution of Data Points by Seasons and Level of Geomagnetic Activity

Geomagnetic Activity	Data Points		Data Points	
	40–60° GMLat	Percent	20–40° GMLat	Percent
<i>Summer</i>				
0–500	4509	51.8	3413	58.3
500–1000	2971	34.2	1669	28.5
1000–2000	980	11.3	648	11.1
2000–4000	237	2.7	129	2.2
subtotal	8697	100.0	5859	100.0
<i>Summer Intermediate</i>				
0–500	3985	62.7	2157	60.8
500–1000	1622	25.5	938	26.5
1000–2000	474	7.5	281	7.9
2000–4000	270	4.3	170	4.8
subtotal	6351	100.0	3546	100.0
<i>Equinox</i>				
0–500	8433	56.0	4583	54.9
500–1000	3436	22.8	1868	22.4
1000–2000	2537	16.8	1457	17.5
2000–3000	658	4.4	440	5.3
subtotal	15064	100.0	8348	100.0
<i>Winter Intermediate</i>				
0–500	2717	49.3	1631	51.5
500–1000	1844	33.4	986	31.2
1000–2000	627	11.4	348	11.0
2000–4000	326	5.9	200	6.3
subtotal	5514	100.0	3165	100.0
<i>Winter</i>				
0–500	5341	58.9	2804	54.9
500–1000	2696	29.7	1605	31.4
1000–2000	928	10.2	606	11.9
2000–4000	108	1.2	90	1.8
subtotal	9073	100.0	5105	100.0
total	44600		26023	

[21] Tables 2a and 2b show the characteristics and the amount and percentages of values contained in each distribution from Figure 3. In Table 2a, the values are separated by season, level of geomagnetic activity, and geomagnetic latitude, and for each season the total number of points used is given. Table 2b offers examples of the kurtosis and skewness for quiet (0–500 units of the integral of *ap*) and perturbed (1000–2000 units of the integral of *ap*) intervals.

[22] The information in Tables 2a and 2b can be helpful to quantify the departure of the distributions of variability from a Gaussian shape. The skewness characterizes the degree of asymmetry of a distribution around its mean. Positive skewness indicates a distribution with an asymmetric tail extending toward more positive values. The kurtosis characterizes the relative peakedness or flatness of a distribution compared to the

normal distribution. Negative kurtosis indicates a relatively flat distribution. For a normal distribution both the kurtosis and the skewness are around zero.

[23] The quiet conditions include more than half of the data, which is generally the case for each particular latitude-seasonal bin. For the quiet condition (0–500, blue line with diamonds in Figure 3), for all seasons and latitudes being discussed, the data typically cover the range from 0.6 to about 1.4 and are distributed around the monthly mean ( $\Phi = 1$ ), with about a third of the population in the center bin ( $\Phi$  between 0.95–1.05).

[24] The low activity intervals for all seasons usually show high values of positive kurtosis (relative peakedness of a distribution compared to the normal distribution) and skewness (degree of asymmetry of a distribution around its mean), representative of a sharp distribution with a significant number of points shifted toward the positive values. The later is possibly related to the definition of the “quiet” interval (0–500), and the consequent inclusion of the small, short-lived positive response at the beginning of the storms [Pröls et al., 1991].

[25] The distributions corresponding to the high levels of activity for summer and equinox (1000–2000 units of the integral of *ap*), with an average population of around 15%, are similar. Both show relatively small values of negative kurtosis and positive skewness, indicating a less sharp distribution with some points

**Table 2b.** Characteristics of the Distributions for Quiet and Perturbed Conditions

	Integral of <i>ap</i> = 0–500		Integral of <i>ap</i> = 1000–1000	
	40–60° GMLat	20–40° GMLat	40–60° GMLat	20–40° GMLat
<i>Summer</i>				
Kurtosis	2.1	1.9	–0.2	–1.2
Skewness	1.7	1.5	1.0	0.1
<i>Summer Intermediate</i>				
Kurtosis	1.9	0.1	–1.1	–0.4
Skewness	1.6	1.1	0.7	1.0
<i>Equinox</i>				
Kurtosis	3.8	2.8	–1.5	–0.8
Skewness	2.0	1.8	0.5	0.8
<i>Winter Intermediate</i>				
Kurtosis	2.5	1.9	–0.1	0.3
Skewness	1.7	1.5	0.827	1.030
<i>Winter</i>				
Kurtosis	3.7	2.4	–0.4	–0.1
Skewness	2.0	1.8	0.9	0.9

QUIET GEOMAGNETIC CONDITIONS (integral of  $ap \leq 500$ )

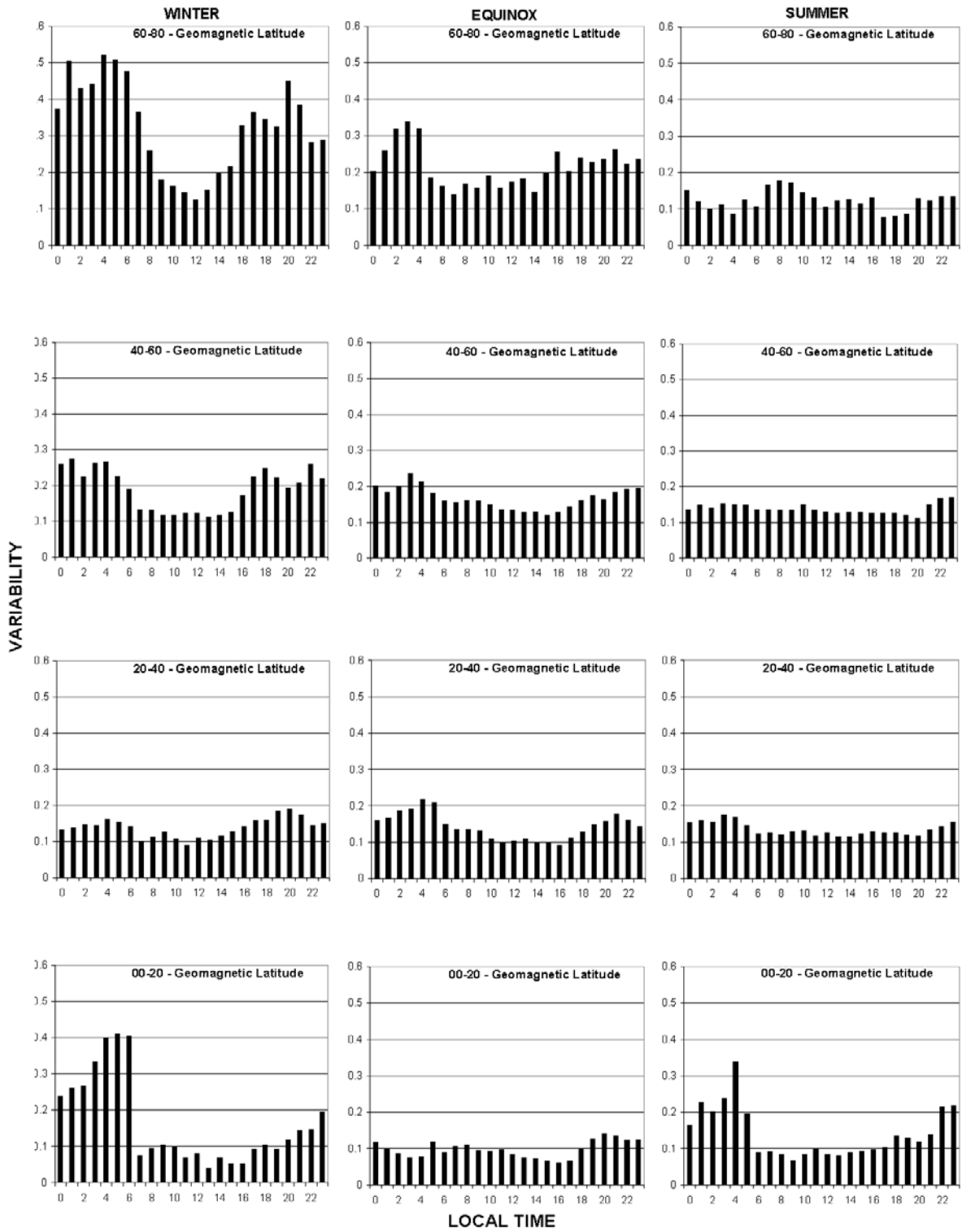


Figure 4

displaced toward values higher than the mean. The same description applies for the higher levels of activity (2000–4000 units) for these seasons, where the average fraction of the population is less than 5%. As expected, the peaks in the distribution move to smaller values as activity increases, signaling the clear negative phase. The exception is summer 20–40°, where at the highest level of activity the distribution is wide and hints at two peaks, one at 0.8 and the second at 0.6. The small population (2.2%; see Table 2a) suggests that it may not be statistically significant.

[26] A comparable picture emerges from the high levels of activity (1000–2000 units) for the winter and winter intermediate seasons. These intervals, with about 11% of the population, have small values of both tests, reflecting a close to normal distribution in each case. As activity increases, the distributions in both bins broaden, becoming more irregular. For 40–60° GMLat, both seasons, there is a trend toward lower values; for 20–40° GMLat winter-intermediate there is a slightly positive shift; and there is very little change for 20–40° GMLat in winter.

[27] There is some hint of a bimodal distribution in some of the winter and winter-intermediate distributions. It is interesting to speculate on the cause of this bimodal distribution. As was discussed earlier, we expect a boundary between the high-latitude region affected by the composition change and the midlatitude and low latitudes where a smaller response is expected. Data recorded on the poleward side would naturally tend to show the negative phase; those on the equatorward side are expected to show small or slightly positive changes. The hint of the two populations may explain the bimodal appearance in Figure 3.

[28] The increase in variability with geomagnetic activity during winter and winter intermediate seasons can also be influenced by the short-lived, fairly localized structures such as storm-enhanced densities (SEDs) [Foster and Vo, 2002]. These features are difficult to capture in the background model so will certainly add to the variability.

### 3.3. Local Time Dependence

[29] The dependence of  $F$  region ionospheric variability on local time is illustrated in Figures 4 and 5. Sufficient data are available to sort the local time variation only at two levels of geomagnetic activity, the quiet bin (integral of  $ap \leq 500$ , Figure 4) and the more active data (integral of  $ap > 500$ , Figure 5). In each level of activity, the variability is shown for three seasons

(winter, equinox, and summer) and for each of the four latitude bands.

[30] The numerical values of the dependence of the ionospheric variability on local time for quiet geomagnetic conditions (integral of  $ap \leq 500$ ) are shown in Table 3. Table 4 shows the corresponding values for disturbed geomagnetic conditions (integral of  $ap > 500$ ). In Tables 3 and 4 the ionospheric variability is organized as a function of the local time and is grouped by the same seasons as Figures 4 and 5.

[31] Several interesting features emerge from the local time dependence of the variability. During geomagnetic quiet conditions at high latitudes, variability is a strong function of local time and season. The variability on the nightside is significantly higher than on the dayside in winter, over 40% compared with less than 20%, while for summer the local time variation has flattened, with values consistently lying between 10 and 15%, and no clear local time dependence.

[32] This picture is consistent with the greater chemical control in summer and the longer daylight hours. The diurnal variation is still evident in the other latitude bands but with smaller amplitude (for example, winter, 20–40° shows around 15% for the night and 10% for the day), and the difference between winter and summer diminishes. At low latitudes the diurnal variation increases in summer and winter and the equinox period stays low. Speculating, the equinoctial minimum at low latitudes, with values in the order of 10%, may be due to the weaker interhemispheric flow, and hence there is a smaller impact of the variable wind systems on the ionosphere.

[33] During the active time (integrated  $ap > 500$ ; see Figure 5 and Table 4), the high latitudes show a clear reduction in variability. This is possibly due to the increased upwelling and increase in neutral molecular species, which tend to impose more chemical control, resulting in lower variability. This implies that structure in the neutral composition has a smaller impact on ionospheric fluctuations than variable winds. In most of the other latitudes and seasons the variability tends to increase with geomagnetic activity. The only exception is the early morning period in winter at low latitudes, where a significant decrease in variability is observed.

## 4. Conclusions

[34] The ionospheric variability for quiet and disturbed conditions has been determined as a function of the local time, geomagnetic activity (expressed in units of the

**Figure 4.** Local time dependence of ionospheric  $F_2$  layer variability, expressed by the standard deviation, for quiet geomagnetic conditions as a function of season and latitude.

**DISTURBED GEOMAGNETIC CONDITIONS (integral of ap > 500)**

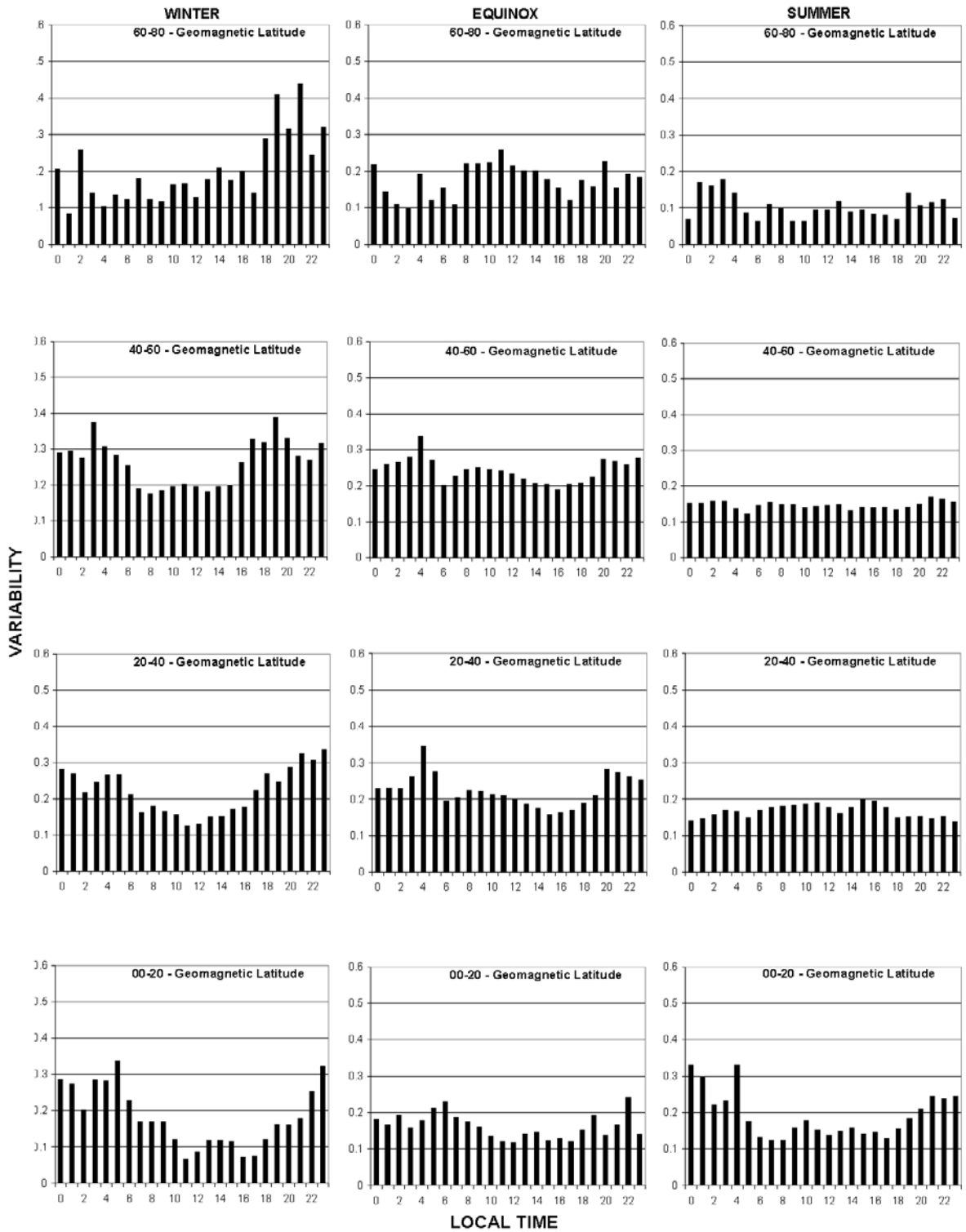


Figure 5. Same as Figure 4 but for disturbed geomagnetic conditions.

**Table 3.** Dependence of the Ionospheric Variability on Local Time for Quiet Conditions

Local Time	Quiet Geomagnetic Conditions (Integral of $ap \leq 500$ )											
	Summer				Equinox				Winter			
	60–80° GMLat	40–60° GMLat	20–40° GMLat	0–20° GMLat	60–80° GMLat	40–60° GMLat	20–40° GMLat	0–20° GMLat	60–80° GMLat	40–60° GMLat	20–40° GMLat	0–20° GMLat
0000	0.15	0.14	0.15	0.16	0.20	0.20	0.16	0.12	0.37	0.26	0.13	0.24
0100	0.12	0.15	0.16	0.23	0.26	0.18	0.17	0.10	0.50	0.27	0.14	0.26
0200	0.10	0.14	0.15	0.20	0.32	0.20	0.19	0.09	0.43	0.22	0.15	0.27
0300	0.11	0.15	0.17	0.24	0.34	0.24	0.19	0.07	0.44	0.26	0.14	0.33
0400	0.09	0.15	0.17	0.34	0.32	0.21	0.22	0.08	0.52	0.27	0.16	0.40
0500	0.13	0.15	0.15	0.20	0.19	0.18	0.21	0.12	0.51	0.23	0.15	0.41
0600	0.11	0.14	0.12	0.09	0.16	0.16	0.15	0.09	0.48	0.19	0.14	0.41
0700	0.17	0.14	0.12	0.09	0.14	0.15	0.13	0.11	0.37	0.13	0.10	0.07
0800	0.18	0.13	0.12	0.09	0.17	0.16	0.14	0.11	0.26	0.13	0.11	0.09
0900	0.17	0.13	0.13	0.07	0.16	0.16	0.13	0.10	0.18	0.12	0.13	0.11
1000	0.14	0.15	0.13	0.08	0.19	0.15	0.11	0.09	0.16	0.12	0.11	0.10
1100	0.13	0.13	0.12	0.10	0.16	0.14	0.10	0.10	0.14	0.12	0.09	0.07
1200	0.11	0.13	0.12	0.09	0.17	0.13	0.10	0.09	0.12	0.12	0.11	0.08
1300	0.12	0.13	0.11	0.08	0.18	0.13	0.11	0.07	0.15	0.11	0.10	0.04
1400	0.13	0.13	0.12	0.09	0.15	0.13	0.10	0.07	0.20	0.12	0.11	0.07
1500	0.12	0.13	0.12	0.09	0.20	0.12	0.10	0.07	0.22	0.13	0.13	0.05
1600	0.13	0.13	0.13	0.10	0.25	0.13	0.09	0.06	0.33	0.17	0.14	0.05
1700	0.08	0.13	0.13	0.10	0.20	0.14	0.11	0.06	0.36	0.22	0.16	0.09
1800	0.08	0.13	0.13	0.13	0.24	0.16	0.13	0.10	0.35	0.25	0.16	0.10
1900	0.09	0.12	0.12	0.13	0.23	0.17	0.15	0.13	0.32	0.22	0.18	0.09
2000	0.13	0.11	0.12	0.12	0.23	0.16	0.16	0.14	0.45	0.19	0.17	0.12
2100	0.12	0.15	0.13	0.14	0.26	0.18	0.18	0.13	0.38	0.21	0.17	0.15
2200	0.13	0.17	0.14	0.21	0.22	0.19	0.16	0.12	0.28	0.26	0.14	0.15
2300	0.13	0.17	0.16	0.22	0.24	0.19	0.14	0.12	0.29	0.22	0.15	0.19

Table 4. Same as Table 3 but for Disturbed Geomagnetic Conditions

Local Time	Disturbed Geomagnetic Conditions (Integral of $ap > 500$ )											
	Summer				Equinox				Winter			
	60–80° GMLat	40–60° GMLat	20–40° GMLat	0–20° GMLat	60–80° GMLat	40–60° GMLat	20–40° GMLat	0–20° GMLat	60–80° GMLat	40–60° GMLat	20–40° GMLat	0–20° GMLat
0000	0.07	0.15	0.14	0.33	0.22	0.25	0.23	0.18	0.20	0.29	0.28	0.29
0100	0.17	0.15	0.15	0.30	0.14	0.26	0.23	0.17	0.08	0.30	0.27	0.27
0200	0.16	0.16	0.16	0.22	0.11	0.27	0.23	0.19	0.26	0.28	0.26	0.20
0300	0.18	0.16	0.17	0.23	0.10	0.28	0.26	0.16	0.14	0.38	0.24	0.29
0400	0.14	0.14	0.17	0.33	0.19	0.34	0.35	0.18	0.10	0.31	0.27	0.28
0500	0.09	0.12	0.15	0.17	0.12	0.27	0.28	0.21	0.14	0.28	0.27	0.34
0600	0.06	0.15	0.17	0.13	0.15	0.20	0.20	0.23	0.12	0.25	0.21	0.23
0700	0.11	0.15	0.18	0.12	0.11	0.23	0.21	0.19	0.18	0.19	0.16	0.17
0800	0.10	0.15	0.18	0.12	0.18	0.25	0.22	0.17	0.12	0.17	0.18	0.17
0900	0.06	0.15	0.18	0.16	0.22	0.25	0.22	0.16	0.12	0.18	0.17	0.17
1000	0.06	0.14	0.19	0.18	0.22	0.19	0.21	0.14	0.16	0.20	0.16	0.12
1100	0.10	0.14	0.19	0.15	0.26	0.24	0.21	0.12	0.17	0.20	0.13	0.07
1200	0.10	0.15	0.18	0.14	0.22	0.23	0.20	0.12	0.13	0.20	0.13	0.09
1300	0.12	0.15	0.16	0.15	0.20	0.22	0.19	0.14	0.18	0.18	0.15	0.12
1400	0.09	0.13	0.18	0.16	0.20	0.21	0.18	0.15	0.21	0.20	0.15	0.12
1500	0.09	0.14	0.20	0.14	0.18	0.20	0.16	0.12	0.17	0.20	0.17	0.11
1600	0.08	0.14	0.19	0.15	0.15	0.19	0.16	0.13	0.20	0.26	0.18	0.07
1700	0.08	0.14	0.18	0.13	0.12	0.20	0.17	0.12	0.14	0.33	0.22	0.07
1800	0.07	0.13	0.15	0.16	0.18	0.21	0.19	0.15	0.29	0.32	0.27	0.12
1900	0.14	0.14	0.15	0.18	0.16	0.22	0.21	0.19	0.41	0.39	0.25	0.16
2000	0.11	0.15	0.15	0.21	0.23	0.27	0.28	0.14	0.32	0.33	0.29	0.16
2100	0.12	0.17	0.15	0.25	0.15	0.27	0.27	0.17	0.44	0.28	0.33	0.18
2200	0.12	0.16	0.15	0.24	0.22	0.25	0.23	0.18	0.25	0.27	0.31	0.25
2300	0.07	0.16	0.14	0.25	0.14	0.26	0.23	0.17	0.32	0.32	0.34	0.32

filtered  $ap$ ), season, and geomagnetic latitude. The first interval of geomagnetic activity, between 0 and 500 units, where more than half of the data lay, corresponds to quiet conditions; the rest of the intervals describe disturbed conditions. Where enough data were available, the standard deviation was used to quantify the ionospheric (observed) variability.

[35] For periods where data were scarce or nonexistent, an estimated variability was provided on the basis of expectations of the consequences of physical processes. This was necessary to fill in the table of values in order to develop a module suitable for inclusion in the International Reference Ionosphere or similar reference models.

[36] During quiet geomagnetic conditions, the lowest variability was found in the summer hemisphere, the maximum in winter, with equinox lying between the two extremes. The exception was at low latitudes, where variability was at a minimum at the equinox. As activity increased, variability decreased at high latitudes and increased elsewhere.

[37] The distribution of the population tended to be Gaussian for most cases, particularly in equinox and summer. In winter the distribution was broader and less well defined and showed evidence for a bimodal distribution in some cases. It is suggested that this may reflect the boundary in neutral composition change expected in the winter hemisphere during storms.

[38] The complete local time sort of the data was restricted to one quiet and one disturbed geomagnetic activity level to ensure statistical significance in the results. The variability showed strong local time dependence, particularly at high latitudes, with nighttime variability always stronger than on the dayside.

[39] A similar study is now being conducted for the ionospheric total electron content (TEC). A database covering a significant number of ionospheric storms is being collected, and from this database a model similar to STORM, but for TEC, will be constructed. This database will also be used to describe the TEC variability for quiet and disturbed conditions.

[40] **Acknowledgments.** National Science Foundation grant ATM-0208069 supported this work. The authors want to thank the unknown referees for their constructive comments.

## References

- Araujo-Pradere, E. A., and T. J. Fuller-Rowell (2001), Evaluation of the STORM Time Ionospheric Empirical Model for the Bastille Day event, *Sol. Phys.*, *204*(1), 317–324.
- Araujo-Pradere, E. A., and T. J. Fuller-Rowell (2002), STORM: An empirical storm-time ionospheric correction model: 2. Validation, *Radio Sci.*, *37*(5), 1071, doi:10.1029/2002RS002620.
- Araujo-Pradere, E. A., T. J. Fuller-Rowell, and M. V. Codrescu (2002), STORM: An empirical storm-time ionospheric correction model: 1. Model description, *Radio Sci.*, *37*(5), 1070, doi:10.1029/2001RS002467.
- Araujo-Pradere, E. A., T. J. Fuller-Rowell, M. V. Codrescu, and A. Anghel (2003a), Evaluation and prospects for storm-time correction in the International Reference Ionosphere (IRI), *Adv. Space Res.*, *33*, 902–909, doi:10.1016/j.asr.2003.07.010.
- Araujo-Pradere, E. A., T. J. Fuller-Rowell, and D. Bilitza (2003b), Validation of the STORM response in IRI2000, *J. Geophys. Res.*, *108*(A3), 1120, doi:10.1029/2002JA009720.
- Araujo-Pradere, E. A., T. J. Fuller-Rowell, and D. Bilitza (2004a), Ionospheric variability for quiet and perturbed conditions, *Adv. Space Res.*, *34*(9), 1914–1921, doi:10.1016/j.asr.2004.06.007.
- Araujo-Pradere, E. A., T. J. Fuller-Rowell, and D. Bilitza (2004b), Time Empirical Ionospheric Correction Model (STORM) response in IRI2000 and challenges for empirical modeling in the future, *Radio Sci.*, *39*, RS1S24, doi:10.1029/2002RS002805.
- Bilitza, D. (2001), International Reference Ionosphere 2000, *Radio Sci.*, *36*(2), 261–275.
- Foster, J. C., and H. B. Vo (2002), Average characteristics and activity dependence of the subauroral polarization stream, *J. Geophys. Res.*, *107*(A12), 1475, doi:10.1029/2002JA009409.
- Fuller-Rowell, T. J., D. Rees, S. Quegan, R. J. Moffett, and G. J. Bailey (1987), Interactions between neutral thermosphere composition and the polar ionosphere using a coupled ionosphere-thermosphere model, *J. Geophys. Res.*, *92*, 7744–7748.
- Fuller-Rowell, T. J., D. Rees, S. Quegan, R. J. Moffett, M. V. Codrescu, and G. H. Millward (1996), A coupled thermosphere-ionosphere model (CTIM), in *STEP Handbook*, edited by R. W. Schunk, pp. 217–238, Utah State Univ., Logan, Utah.
- Fuller-Rowell, T. J., M. V. Codrescu, and E. A. Araujo-Pradere (2001), Capturing the storm-time ionospheric response in an empirical model, in *Space Weather, Geophys. Monogr. Ser.*, vol. 125, edited by P. Song, H. Singer, and G. Siscoe, pp. 393–401, AGU, Washington, D. C.
- Millward, G. H., H. Rishbeth, T. J. Fuller-Rowell, A. D. Aylward, S. Quegan, and R. J. Moffett (1996), Ionospheric  $F_2$  layer seasonal and semiannual variations, *J. Geophys. Res.*, *101*, 5149–5156.
- Pröls, G. W., L. H. Brace, H. G. Mayr, G. R. Carignan, T. L. Killeen, and J. A. Klobuchar (1991), Ionospheric storm effects at subauroral latitudes: A case study, *J. Geophys. Res.*, *96*, 1275–1288.
- Quegan, S., G. J. Bailey, R. J. Moffett, R. A. Heelis, T. J. Fuller-Rowell, D. Rees, and R. W. Spiro (1982), A theoretical study of the distribution of ionization in the high-latitude ionosphere and the plasmasphere: First results on the midlatitude trough and the light-ion trough, *J. Atmos. Terr. Phys.*, *44*, 619–640.

- Richmond, A. D., E. C. Ridley, and R. G. Roble (1992), A thermosphere/ionosphere general circulation model with coupled electrodynamic, *Geophys. Res. Lett.*, *19*, 601–604.
- Roble, R. G. (1986), Chemistry in the thermosphere and ionosphere, *Chem. Eng. News*, *64*(24), 23–28.
- Roble, R. G., E. C. Ridley, A. D. Richmond, and R. E. Dickinson (1988), A coupled thermosphere/ionosphere general circulation model, *Geophys. Res. Lett.*, *15*, 1325–1328.
- Schunk, R. W., J. J. Sojka, and M. D. Bowline (1986), Theoretical study of the electron temperature in the high latitude ionosphere for solar maximum and winter conditions, *J. Geophys. Res.*, *91*, 12,041–12,054.
- 
- E. A. Araujo-Pradere, T. J. Fuller-Rowell, and M. V. Codrescu, Cooperative Institute for Research in Environmental Sciences, University of Colorado, and SEC, NOAA, 325 Broadway R/SEC, Boulder, CO 80305, USA. (eduardo.araujo@noaa.gov)
- D. Bilitza, Raytheon ITSS/NASA Goddard Space Flight Center, Code 632, Greenbelt, MD 20771, USA.